Electron Reflection Coefficient at Zero Energy. II. Computer Experiments on the Reflection of Slow Electrons in the Electrostatic Field of Surface Patches*

H. HEIL
Hughes Research Laboratories, Malibu, California
(Received 19 June 1967)

As reported in paper I, the zero-energy reflection coefficient of electrons at a polycrystalline silver surface has been measured to be (7±1)%. A theory consistent with this experimental result is presented below. This theory shows that the zero-energy reflection coefficient may be fully explained by the effect of patches of different work functions. The different potentials presented at the surface of a metal by the differently oriented crystal surfaces converge exponentially to the average potential as one moves away from the surface. The potential variation with the largest spatial period extends farthest from the surface. It will be shown that this component alone determines the reflection behavior at the threshold of energy. Because the surface presents a two-dimensional distribution, two independent periods must be considered which range in their aspect ratio from a square checkerboard to long stripes. The reflection coefficient is found to be independent of patch size and patch potential amplitude, and is (7.73±0.03)% for the stripe-type and (5.4±0.2)% for the square-checkerboard-type patches. The reflection coefficient jumps abruptly from 100% below the threshold of energy to some 6% at an energy immediately above threshold; therefore, It is not surprising that recent energy analyses with a simple patchy counterfield electrode of several-hundred-millivolt patch amplitude can resolve fine structure in the energy of less than 10 meV, as exhibited in the energy spectrum of electrons field-emitted from a liquid-helium-cooled tip.

I. INTRODUCTION

THE surface of a solid which is not a single crystal shows a variety of differently oriented crystallite surfaces with different work functions. The resulting surface patches may range from a few tens of nanometers to several micrometers in diameter and may cause a variation of the potential along the surface of more than 1 V. These variations are known to be strongly affected by an adsorbed layer (especially of alkali atoms).

In the plane of the surface (x,y) the potential $P(x,y)$ may be described by a two-dimensional series summed over n and m with terms such as $a_n \sin(nx/x_0)b_m \times\sin(my/y_0)$. Here x and y are the coordinates along the surface, x_0 and y_0 are the lengths of the fundamental periods, and the complex numbers a_n and b_m are the amplitudes and phases of the particular component. There are nm such components. The dependence of P on the third dimension z perpendicular to the surface is found by satisfying Laplace's equation $\Delta P(x,y,z)=0$, which holds in the absence of space charge. A simple exponential decrease $\exp[-(n^2/x_0^2+m^2/y_0^2)^{1/2}z]$ results for the n-m term. One sees that the term which reaches farthest from the surface, or dies off most slowly, is the one with $n=m=1$. The fields from this term are those felt first by an approaching electron, and they primarily determine the behavior at threshold of energy. In the following, we shall investigate electron trajectories in the three simple potentials:

$$\begin{aligned}&\text{(a)}\ P(x,y,z)=\sin x e^{-z},\\ &\text{(b)}\ P(x,y,z)=0.5\sqrt{2}[\sin x e^{-z}+\sin(2x+p)e^{-2z}],\\ &\text{(c)}\ P(x,y,z)=\sin x \sin y e^{-\sqrt{2}z}.\end{aligned} \quad (1)$$

Here (a) represents simple sinusoidal stripes, (b) stripes with the first harmonic added at equal amplitude and different phases p, and (c) a simple sinusoidal, quadratic checkerboard.[1]

The nature of the patches themselves has recently become the subject of experimental research. The actual size and potential excursion of patches can be determined by a method which is essentially a refinement of the camera-tube technique of reading small charge deposits by means of a magnetically focused, low-energy electron beam. To resolve the smaller patches, the beam must be focused to a small spot (≈1 μm); at the same time, the electric field applied to the surface must be increased beyond a value obtained by dividing the patch potential amplitude by the beam diameter. This limits the experimental method, presently at about 2-μm spatial resolution, 10-mV potential resolution, and 4-kV cm^{-1} applied field. With ingenious data-processing methods, patch distribution functions have been recorded directly and their dependence on temperature and adsorption may be studied.[2]

Early interest in the reflection of electrons by patch fields arose in connection with the study of thermal-electron emission and how it is affected by the reflection of the outgoing electrons. The reflection coefficients for ingoing and outgoing electrons are simply related; the relation can be obtained by considering an electron gas in thermal equilibrium and in contact with the emitter. Following the principle of detailed balancing, corresponding (in direction and energy) electron fluxes through the boundary between the two phases are equated. Only the reflection coefficient for ingoing electrons offers the possibility of experimental determi-

* Work partially supported by U. S. Air Force Cambridge Research Laboratories under Contract No. AF 19(628)-4297.

[1] A more detailed description of these potentials is found in C. Herring and M. H. Nichols, Rev. Mod. Phys. 21, 185 (1949) Appendix IV.

[2] G. A. Haas and R. E. Thomas, Surface Sci. 4, 64 (1966).

nation. For truly thermal energies, even this is quite difficult, as evidenced in the preceding paper.[3] In their survey article on thermionic emission, Herring and Nichols[4] have given a qualitative analysis of the reflection of electrons by patch fields as Appendix V. A geometrical consideration in the phase space of the initial coordinates and momenta gives some insight into the behavior of the reflection coefficient at the onset of reflection. No trajectory computations were made, presumably because computers were not as practical in use at that time. The use of the simplified potentials [Eq. (1)] is suggested there.

A more serious need for the knowledge of the electron-reflection coefficient associated with the patch field at a surface arises when a counterfield method is used to obtain an energy spectrum of a beam. In this method, the electron beam to be investigated is directed toward a decelerating electrode; care is taken to collimate the beam well in order to obtain the total energy. The current acceptance by the counterfield electrode as a function of the potential applied to the same electrode is plotted, and the differential quotient of that curve represents the energy spectrum. The difficulty arises when one strives for an energy resolution (e.g., 30 meV) which is smaller than the patch potential variation (e.g., 300 mV) over the surface of the counterfield electrode.[5] How many of the electrons which overcame the average potential above the patches are really returned by the more negative patches, and how does that reflected part depend on the energy above the threshold? From observations in which relatively sharp features are expected in the electron energy spectrum (such as the field-emitted electrons from a cooled tip), it appears that the patchy surface behaves as a unipotential surface. This is demonstrated by the experiments of Young and Muller,[6] Holscher,[7] and von Oostrom.[8]

The numerical calculations of this paper will show that the channeling of the electrons into the more positive patches is such that at threshold of energy, only between 5.4 and 7.7% of the electrons are reflected, and this percentage is independent of patch size and patch potential variation. Although this holds exactly only for orthogonal incidence and small applied field, it also has been found to be approximately correct for a large range of nonorthogonal angles of incidence ($\pm 25°$) and for moderately strong applied fields (about 10^{-3} of patch field). In addition, we find that the small reflection coefficient remains fairly constant with energy above threshold. Finally, from calculations over the full range of oblique incidence, we compute the average reflection coefficient for a distribution which is completely isotropically incident to the surface. This value, which was found to be 20%, also holds for a Maxwellian, provided kT/e is smaller than the patch potential amplitude.

II. TRAJECTORY CALCULATIONS

Assume that a beam of electrons is directed toward the surface; the beam is parallel and of uniform density, and all electrons have the same energy of such magnitude that only part of the surface can be energetically reached by them. There will be deflections and reflections, which are dependent on where the electron enters the field. The general character of the deflections will be such that reflections will occur above the most negative patches, and electrons are deflected and channeled into the more positive patches of the surface between the positive and negative patches.

At a sufficiently large distance z_0 from the surface, the patch field is negligibly small and the trajectories are straight or very slightly curved parabolas if there is an applied field. Let us characterize the position at which the electron enters by x_0 and y_0. If we then study the trajectories as a function of this position (x_0,y_0) we shall find certain areas from which the electrons are accepted (i.e., $z<0$) and we shall find such coordinates x_0, y_0 for which the electron is returned (i.e., $z>z_0$). The reflection coefficient is then found simply by counting the area from which electrons were reflected and dividing it by the total area in the x_0-y_0 plane.

In earlier attempts to carry out such calculations, C. Buckey and the author used the electrolytic tank and analog computer to trace the trajectories. However, it was soon learned that the analog computer was not sufficiently accurate and that the bookkeeping and data processing of the many trajectories were prohibitively laborious. Furthermore, one would be limited to two-dimensional potentials only.

The potentials to be considered here appear as

[3] See H. Heil and J. V. Hollweg, preceding paper, Phys. Rev. **164**, 881 (1967); referred to as I.

[4] C. Herring and M. H. Nichols, Rev. Mod. Phys. **21**, 185 (1949), Appendices V, Va, and Vb.

[5] If this electrode is in the form of a mesh and only the current which passes through the mesh openings is used to derive the energy spectrum, as has been done [H. Heil and B. W. Scott, U. S. Air Force Scientific Report No. AFCRL-66-769, 1966 (unpublished) (available from CFSTI, 5285 Port Royal Road, Springfield, Virginia); H. Heil, Bull. Am. Phys. Soc. **7**, 488 (1962)] and is described in I (Ref. 3), the surface potential variations have died off sufficiently that they do not have any effect on the potential over the mesh opening, and the spectrometer can work with an energy resolution in excess of the patch potential variation.

[6] R. D. Young and E. W. Müller, Phys. Rev. **113**, 115 (1959).

[7] A. A. Holscher, Surface Sci. **4**, 89 (1966); the energy distribution function has a sharp edge at the high-energy end, representing the Fermi level. The electrons arrive quite orthogonally, the stated energy resolution is 0.03 eV; the applied field is 70 V cm^{-1}; the patches are assumed to vary by several tenths of a volt, to have a size of 10^{-5} cm, and to produce a field of 10^4 V cm^{-1}. Note the first paragraph on p. 99 for the qualitative arguments for the smallness and constancy of the patch-reflection coefficient.

[8] A. van Oostrom, Philips Res. Rept., Suppl. **1**, 1 (1966); see second paragraph p. 54 and Fig. 3.26 on p. 55 for a demonstration of a resolution better than 10 meV with the tip at liquid-helium temperature. The collector is a hemisphere made of polycrystalline molybdenum or nickel, for which the patch amplitude far exceeds 10 mV.

exponential and trigonometric functions only, suggesting the use of a digital computer with its much higher accuracy and speed, and its greater ability of data digestion and selection. In this case a trajectory calculation simply consists first in defining the three initial coordinates, the three initial velocity components, and a time step; and second in increasing each coordinate by the product of the time step and the particular velocity component, and in increasing the velocity components by the product of the same time step and the particular acceleration component or force component, which in turn is computed directly from the analytical expression of the potential. The size of the time step is chosen so small that further reduction no longer changes the trajectory.[9] From 100 to 1000 steps per trajectory were sufficient, and the computer time per step was 10 msec. The computation is interrupted if $z<0$ (accepted) or if $z>z_0$ (reflected), and the initial coordinate x_0 is changed until a value is reached for which a change occurs from acceptance to reflection. This x_0 value is stored, and after completion of a complete period, the percentage of electrons reflected is computed. The initial energy of the electron is characterized by three energy components (the squares of the three initial velocity components). The amount of applied field which is to be added to the patch field appears simply as a term Az in the potential. Since the scale for time is arbitrary, we set the field components directly equal to the components of acceleration. This implies that $e/m=1$.

By far, the simplest potential is the one-dimensional periodic potential $\sin x \exp(-z)$. Calculations with it reveal most of the characteristic features, and we shall therefore discuss it in detail below.

III. THE POTENTIAL $\sin(x)e^{-z}+Az$

This potential is depicted in Fig. 1. Since it is a function of only two coordinates x and z, it can be represented in a perspective drawing. At the surface ($z=0$) the patch potential amplitude is taken to be unity (1 V). The period does not affect the reflection coefficient and it is chosen such that the patch-field amplitude is also unity. The applied field A is taken to be about 5% of the patch field amplitude. The line crests and valleys are marked, as well as the straight potential lines which run along the steepest lateral slope. Along the valley line a saddle point appears the position z_s at which depends on A as $z_s=-\ln A$ and the potential of which $P_s=A(1-\ln A)$. In the absence of an applied field, this point disappears: $z_s\to\infty$. In the lower part of Fig. 1, we show the potential as a function of the distance from the surface z for the case where the applied field $A=10^{-3}$. In this case, the saddle point appears at the position $z_s=6.92$ and its potential has the value 7.91 mV. For the start of the trajectory we choose $z_0=14$; at this position the potential variation along x is about 1 μV. In later calculations the initial value $z_0=9$ was found to be sufficiently distant from the surface.

In Fig. 2, we show a variety of trajectories with orthogonal incidence. One looks onto the z-x plane; the saddle point is marked, as are the lines along the crest and the valley of the potential, and the lines midway between these extremes. For each position x_0 at the launch line, one can find an energy value for which the trajectory changes from accepted to reflected or vice versa; this is called the critical energy. We show five such positions x_0 between the valley and crest on the left side, and we indicate the critical energy value in meV below the launch line. One sees that energies slightly below zero (i.e., below the energy necessary to reach the average potential) are already sufficient. This results because of the suppression of P at the saddle point by 7.91 mV below the average value; one sees indeed that all of the nine trajectories pass close to that point. Those trajectories are deflected into the valley and complete one or several oscillations in it. As the x_0 value for the crest is approached, substantially more initial energy is necessary for the trajectory to be accepted. The trajectory shown on the left has a critical energy of 940 meV (i.e., nearly sufficient to reach the most negative part of the surface). The character of this trajectory is discussed in detail in Sec. IV.

If the critical energy listed below the launch line were drawn as a function of x_0, one would find a very slight change with x_0 up to a value of $x_0=-1.325$. At this value, the critical energy would rise very steeply to a value approaching 1. The corresponding trajectory runs essentially along a line close to and parallel to the crest line; it then turns sharply into the valley and either is reflected or enters into the surface. This was surprising and led to the investigation of the more ideal case of zero applied field ($A=0$). In this case, the critical energy is zero for all values of x_0 up to $x_0=-1.325$, at which value the critical energy rises abruptly from zero to a value close to one. After demonstration of this fact by numerical computations, we also were able to prove it analytically. In the next section, we consider this case, and we shall find a general property of trajectories entering a potential generated from a potential distribution over a plane surface. This theorem will greatly reduce the amount of computation necessary and will allow us to state a simple threshold law for the reflection coefficient.

[9] A program in which the time step was varied in accordance with the absolute value of the acceleration showed that the number of trajectory steps could be reduced; however, the time-step calculation itself lengthened the computer time more than the possible reduction in the required total number of steps would shorten it.

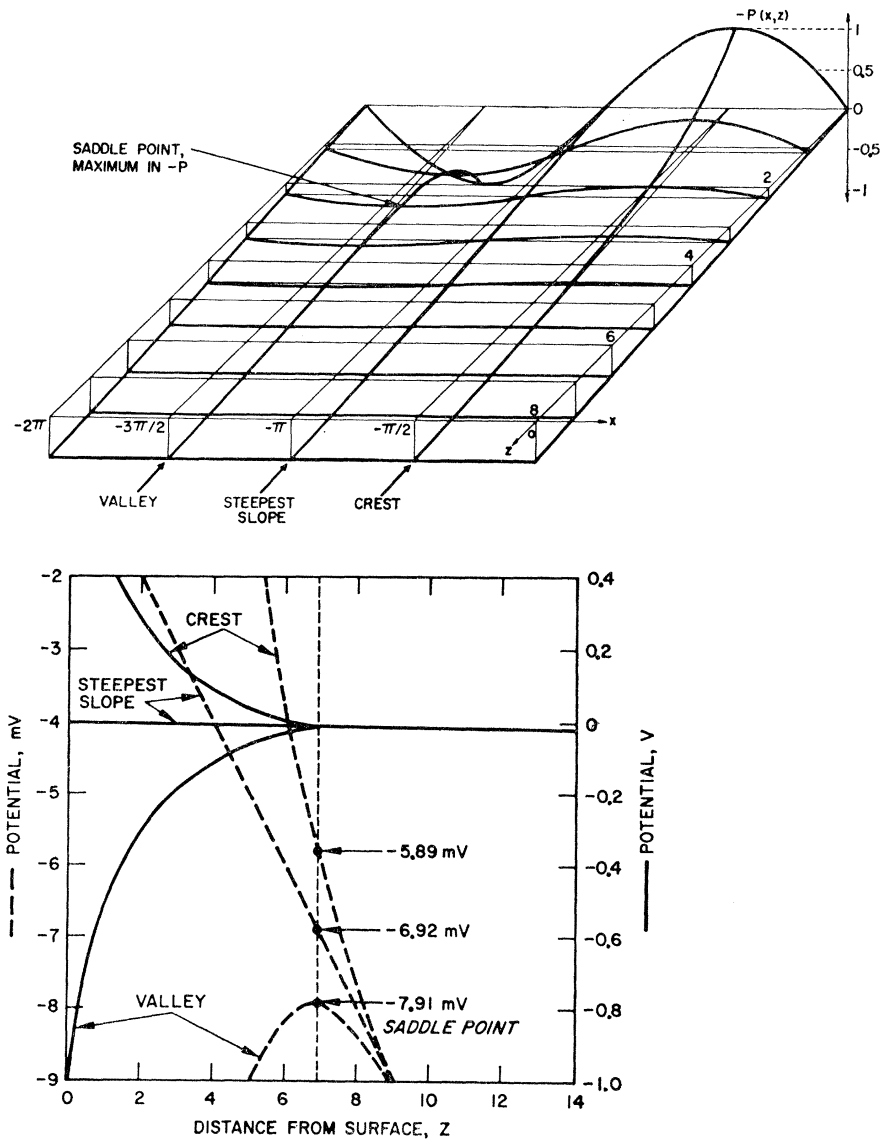

FIG. 1. (a) The negative of the potential $P(x,y,z)=\sin(x)e^{-z}+0.05z$ shown above the x-y plane; one may picture electrons entering the terrain in the direction of the arrows going uphill and with an energy approaching that which is necessary to climb the zero line at the surface. (b) The negative of the potential $P(x,y,z)=\sin(x)e^{-z}+10^{-3}z$ showing detail of the potential around the saddle point which is at $z_s=6.92$ and along $x=-\frac{3}{2}\pi$ (valley), as well as along $x=-\pi$ (steepest slope) and $x=-\frac{1}{2}\pi$ (crest); the three dashed lines correspond to the mV scale at the left. The negative of $P(x,y,z)$ is chosen in order to convey the impression of a particle moving in a terrain under the influence of earth's gravity.

IV. REFLECTION COEFFICIENT AT THRESHOLD; GENERAL PROPERTIES OF TRAJECTORIES ENTERING A POTENTIAL GENERATED BY A POTENTIAL DISTRIBUTION AT A SURFACE

The critical trajectory for normal incidence and at zero applied field occurs at $x_0=-1.325$ (that is, 13°55′ away from the crest line) and implies a percentage of reflection of $7.73\pm0.03\%$. This trajectory is shown in the x-z plane in Fig. 3. The regions of reflection are marked by hatches. Three trajectories are shown, two starting at $x_0=-1.326$ with energies of 0.1 and 0.4 eV.[10] Both are reflecting trajectories. The third trajectory—an accepting one—starts at $x_0=-1.324$ with the energy of 0.4 eV. A closer inspection of the very narrow transition region $-1.324>x_0>-1.326$ shows that trajectories between these two limits make several oscillations within the valley before they leave either to the left or to the right in reflection or into the surface.

It is apparent that the two reflecting trajectories are identical except for a displacement in the z direction. In order to prove this, consider a trajectory determined by the three initial coordinates and velocities $(x_0,y_0,z_0,\dot{x}_0,\dot{y}_0,\dot{z}_0)$ in a potential $P(x,y,z)$. Consider next a trajectory which starts at the same point (x_0,y_0,z_0) in a potential which is m times larger $mP(x,y,z)$. The second trajectory is identical to the first, provided that the initial velocities $\dot{x}_0$, $\dot{y}_0$, $\dot{z}_0$ are multiplied by the factor $m^{1/2}$, or the components of the initial energy by the factor m. This is equivalent to the well-known fact in electron optics that trajectories depend only on the

[10] The energy in electron volts implies that the patch-potential amplitude at the surface is normalized to 1 V.

ratio of the applied voltages (if those are referred to the emitter potential). Only the time scale for the new trajectory is changed by a factor $m^{-1/2}$. On the other hand, multiplication of the specific potential of Fig. 3 by the constant factor m can also be obtained by a translation of the coordinate system in the z direction by $\bar{z}=\ln(m)$. Indeed, we see that the parallel shift between the two trajectories in Fig. 3 is of the proper magnitude [viz., $\ln(4)$].

More generally, for a potential of the form

$$P(x,y,z)=P_1(x,y)e^{-lz}, \tag{2}$$

the multiplication by a constant m is equivalent to a translation of the coordinate system in the z direction:

$$mP(x,y,z)=P_1(x,y)\exp[-l(z-\bar{z})]$$
$$=\exp(l\bar{z})P(x,y,z), \tag{3}$$

where $\bar{z}=\ln(m)/l$. A trajectory in the potential (2) which is represented by $x(t)$, $y(t)$, $z(t)$ reads, in the new potential (3), $x(m^{-1/2}t)$, $y(m^{-1/2}t)$, $z(m^{-1/2}t)+\bar{z}$.

In all trajectories considered in this paper the initial position x_0, y_0, z_0 is well outside the influence of the potential [$P(x_0,y_0,z_0)<10^{-6}$ V]. Consequently, a change of the initial energy always results in a simple z shift of the trajectory and, specifically, the property of a trajectory of being critical is not affected. Only when the initial energy is increased close to unity does the turning-around point of the critical trajectory of Fig. 3 pass through $z=0$, which leads to acceptance. Thus, the dependence of the acceptance coefficient on energy

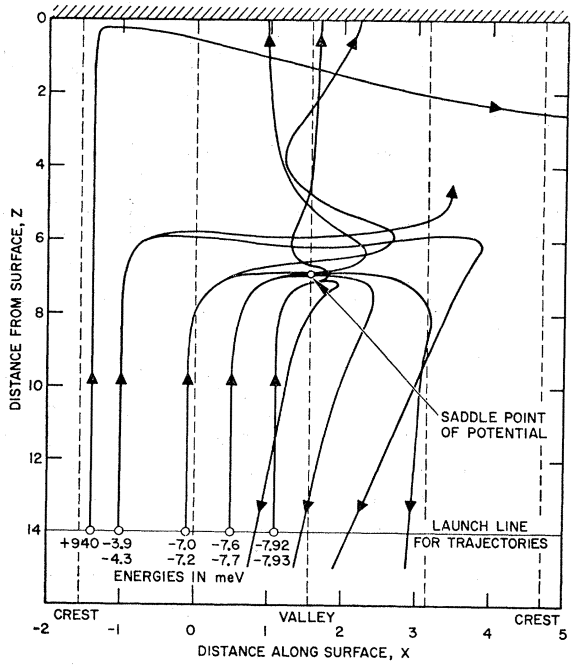

FIG. 2. Critical trajectories in the x-z plane in the potential $P(x,y,z)=\sin(x)e^{-z}+10^{-3}z$, orthogonal incidence; five launch positions with the respective critical energies.

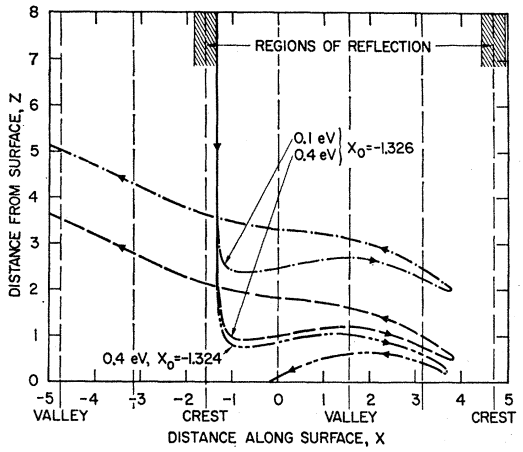

FIG. 3. Three critical trajectories in the x-z plane in the potential $P(x,y,z)=\sin(x)e^{-z}$, orthogonal incidence; two initial energies: 0.1 and 0.4 eV. Note that the two reflecting trajectories are identical, but displaced by $\ln(4)$ in the z direction and that the exactly critical trajectory comes to a point ($x\approx3.8$) where the velocity goes through zero.

is quite simple. The coefficient is zero for energies below that sufficient to reach the average potential (called zero in Fig. 8); it then rises abruptly to 92.27% and stays constant at this value up to an energy which is sufficient to reach the most negative surface potential (−1 V); it then rises to 100% or full acceptance. (The fashion in which the transition to 100% occurs is dependent upon the higher harmonics in the potential. It is not considered in detail here. Some consideration was given to this detail by Herring and Nichols.[4]) It is the abrupt rise from zero to 92.27% at the threshold energy which makes the high-resolution measurement[6,7,8] understandable.

It should be emphasized that the fact that the critical character of the trajectory is independent of energy applies to all potentials of the type (2), where $P_1(x,y)$ is an arbitrary function of x and y, and l is a real constant. Therefore, it applies to the fundamental of the simple stripe-type potential and to the checkerboard-type potential of any arbitrary aspect ratio of the fundamental checkerboard rectangle. However, it does not apply to potentials with an applied field superimposed, or at least it applies only approximately in this case, as we have seen in Sec. III.[11] It also does not apply to potentials which consist of a sum of terms with different l's. Regarding the latter case, however, we note that one can always find a low enough energy, such that the trajectory turning point occurs at a position so far from the surface that the terms with the larger l values have a negligible effect on the trajectory. Therefore, the reflection coefficient at threshold, and the abrupt rise there, are quite independent of the amplitudes of the higher harmonics,

[11] For an applied-field–to–patch-field ratio of 10^{-3}, the sharp corners in Fig. 8 are rounded so little that it would not be visible in this figure. The extension into energies below zero is 7.9 meV at the most.

i.e., of the detailed nature of the patches. The value is 7.73% for the stripe-type potential and, as we will see later, 5.4% for the square checkerboard-type potential. For patches which have a rectangular rather than square fundamental range, one may expect a value between those two numbers.

V. OBLIQUE INCIDENCE FOR THE POTENTIAL $\sin(x)e^{-z}$

Since the acceptance coefficient $\sin(x)e^{-z}$ does not depend on the energy, its dependence on the angle of incidence is a function of some generality and was therefore calculated. Call the angle of incidence α_x, defined by $\alpha_x \equiv \dot{x}_0/\dot{z}_0$. As we saw in the case of orthogonal incidence in Figs. 2 and 3, the reflection is not specular, and no simple relation exists between angle of exit and angle of entry. A program was written which computes the fraction of the initial coordinates x_0 from which the electrons are accepted. The result, the function $A(\alpha_x)$, is shown in Fig. 4 in a polar diagram. $A(\alpha_x)$ is fairly constant for the first 20° around orthogonal incidence; it then drops off suddenly for α_x toward 70° and is zero from 70° to 90°, a range where total reflection occurs. In Fig. 4 we also show the acceptance $A(\alpha_y)$, i.e., if $\dot{x}_0=0$ but $\dot{y}_0$ is varied, and $\alpha_y \equiv \dot{y}_0/\dot{z}_0$. $A(\alpha_y)$ is independent of α_y and has the value 92.3%.

For the more general case of a combination of initial x and y motion, one can ask for an average acceptance function $A(\alpha)$, where α is the polar angle off the perpendicular to the x-y plane as defined in the insert to Fig. 4. It is necessary to introduce the azimuthal angle λ as shown and compute an average between $A(\alpha_x)$ and $A(\alpha_y)$ through all λ's. The result is also shown in Fig. 4.

Finally, for a completely isotropic electron flow incident to the surface, one must average $A(\alpha)$ over all α's equally weighted, obtaining the value $A_0=80\%$ for the average acceptance coefficient. This is the value which applies to a Maxwellian. The more orthogonal part is almost entirely accepted, while the part with more grazing incidence is almost entirely reflected. However, the principle of detailed balancing must be applied carefully for the purpose of drawing conclusions concerning the reflection coefficient applicable in electron emission. While the average value A_0 is also applicable as a transmission coefficient for emission, the angular dependence is not determined by the angle of reflection. Since the reflection is not specular, these latter angles are not known. During the computation it was noticed that when that position in x_0 was approached at which the trajectory turns critical, the angle of exit changed very rapidly between the limits of about ±70°. The only fact which can be readily stated about the angular distribution of thermally emitted electrons from a patchy surface (in the absence of space charge) is that there is a deficiency in emission at large angles α (i.e., parallel to the surface). This deficiency can be seen experimentally in retarding potential measurements of the axial energy,[12] where it manifests itself as a "rounding of the upper knee." Total energy spectra[13] do not show any change in shape if the angular distribution of the emitted current is incomplete.

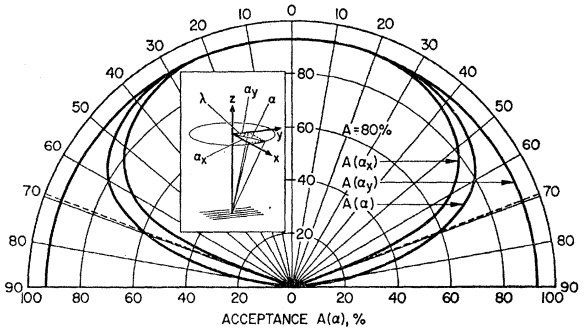

FIG. 4. Polar diagram for the acceptance coefficient A as a function of angle of incidence in the potential $P(x,y,z)=\sin(x)e^{-z}$. The three angles α_x, α_y, and α are defined with respect to the stripe direction in the insert; λ, azimuthal angle; for a definition of $A(\alpha_x)$, $A(\alpha_y)$, $A(\alpha)$, and A, see text.

We give now some samples of acceptance coefficients for a potential with the first harmonic added at equal amplitude, but with different phases.

VI. THE POTENTIAL $0.5\sqrt{2}[\sin(x)e^{-z}+\sin(2x+p)e^{-2z}]$

From the many possible combinations with the first harmonic, we select a combination with equal amplitudes of $0.5\sqrt{2}$ V and four different phases, namely $p=0$, 1, 3, 5 rad. We calculate the critical energy as function of x_0 and show the result in Figs. 5(a) and 5(b), all for orthogonal incidence only. At the threshold of energy, the regions of reflection are located at the crests of the fundamental, as we had expected from the analysis in Sec. IV. With increasing energy, the regions then move over to the position of the crests of the first harmonic. This movement would have been more complete if we had defined the acceptance by a more negative value of z than zero (which is equivalent to increasing the amplitude of the first harmonic with respect to the fundamental).

The width of the reflected region is first constant and equal to the case of the fundamental alone; at higher energies, the range generally narrows. For the case of $p=5$ rad, it first widens, branches into two regions, and then vanishes at about half that energy, at which it vanishes in the other cases.

In Fig. 6, we show the acceptance functions for three cases and the fundamental. The case $p=0$ rad is deleted because it is quite similar to $p=3$ rad. Also

[12] H. Shelton, Phys. Rev. **107**, 1553 (1957); P. Kisliuk, *ibid.* **122**, 405 (1961); for an analysis of incomplete angular distribution functions, see Heil and Scott (Ref. 5) and Heil (Ref. 5).
[13] See Heil and Scott, Ref. 5; Heil, Ref. 5.

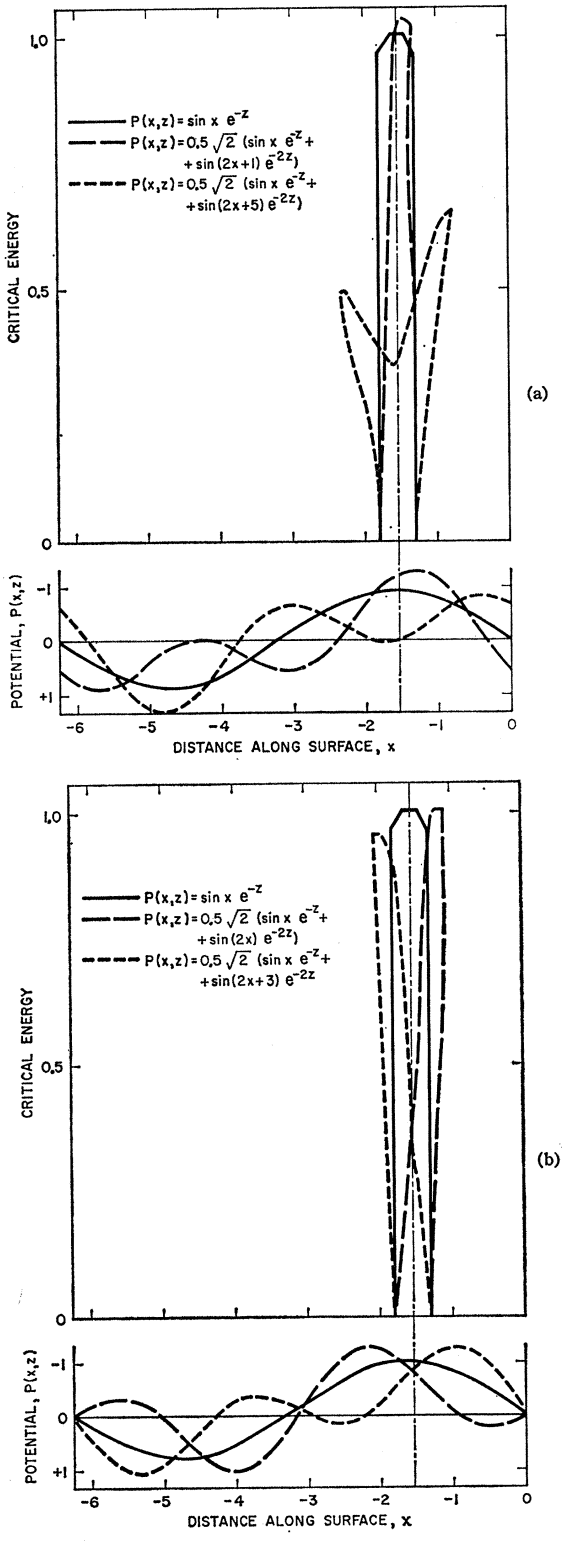

FIG. 5. Plots of critical energy (upper parts) and surface potential (lower parts) over one full period of the entrance phase x_0; in addition to the case of the simple function $P(x,y,z)=\sin(x)e^{-z}$ (solid line), the functions containing also a first harmonic are shown; (a) the case for the first-harmonic phases 0 and 3 rad; (b) for the phases 1 and 5 rad.

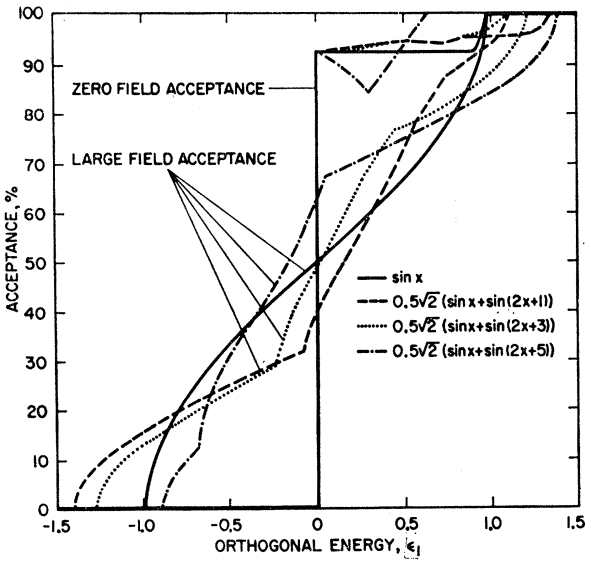

FIG. 6. Acceptance coefficient for three of the cases of Fig. 5 and for the simple case $P(x,y,z)=\sin(x)e^{-z}$ (solid curve); both zero-field and large-field acceptances are computed and plotted.

shown are the acceptance functions for the case where the applied field is so large that deflections in the patch field can be neglected entirely.

VII. THE QUADRATIC CHECKERBOARD POTENTIAL $\sin(x)\sin(y)e^{-\sqrt{2}z}$, NORMAL INCIDENCE ONLY

The additional dimension does not greatly complicate the trajectory computation, but the additional dimension in the initial coordinate causes a laborious integration of the x_0-y_0 area (a star-shaped figure) from which reflection takes place. In Fig. 7 we show over the x-y plane the equipotential lines for the square, $0<x<\pi/2$, and $0<y<\pi/2<y<\pi$ which bounds a positive potential hill (which constitutes one quadrant of the entire fundamental square). In the upper square, $0<x<\pi/2$, and $\pi/2<y<\pi$ (which bounds a potential dale), reflection occurs inside the star-shaped area.

It is of interest to note that trajectories are two-dimensional if they originate at the dashed and at the dotted lines. The potentials in the corresponding planes, including a z dimension, are shown at the very top of the figure. The case of the dashed lines is similar to the simple $\sin(x)e^{-z}$ potential of Sec. IV, except that the exponent is larger by the factor $\sqrt{2}$. The consequent, steeper rise of the potential amplitude with decreasing z makes for a larger reflection range. The range for the potential of Sec. IV is marked by the dash-dotted lines. The planar trajectories along the dotted, diagonal lines are very strange because all

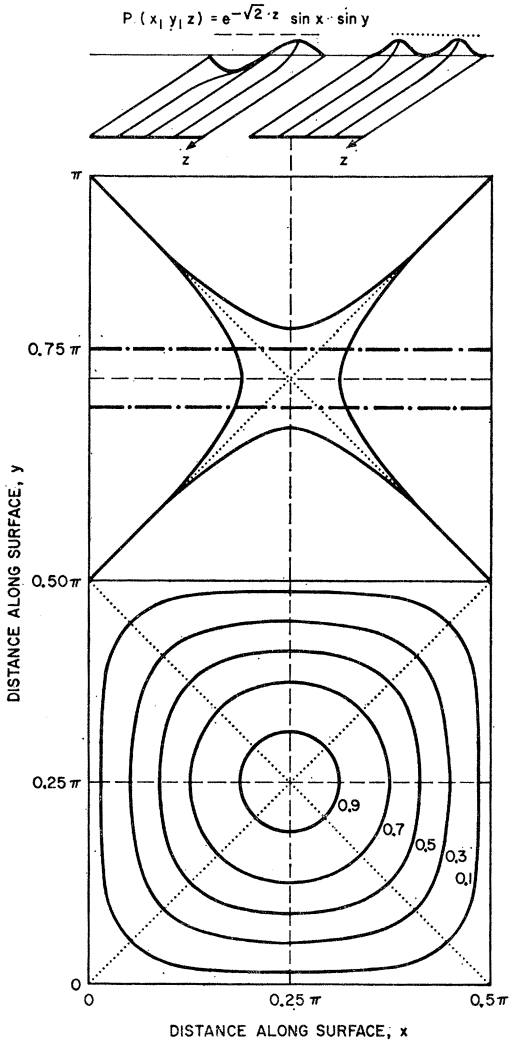

FIG. 7. Two quadrants of the basic square of the checkerboard potential $P(x,y,z)=\sin x \sin y(e^{-\sqrt{2}z})$; for $z=0$, the lower square marks the equipotential lines and the upper square (where $P<0$) marks the star-shaped figure, within which reflection occurs for normal incidence. The dash-dot line marks the reflection-acceptance border for the stripe-type potential; along the dashed and the dotted line, the trajectories remain two-dimensional and the corresponding potential distributions are shown at the top in the fashion of Fig. 1.

trajectories are reflecting. The oscillations in those potential valleys increase until reflection occurs; then they decrease again, similar to the reflection of a plasma by a magnetic field with a cusped geometry.

In Fig. 8, the acceptance curves of the square-checkerboard potential are compared with the stripe-type potential. Orthogonal incidence and only the fundamental period potential are assumed. The large applied-field acceptance curve for the stripe-type potential is also shown; it is a sinusoidal function. The same curve for the square-checkerboard potential has also been integrated numerically and appears as the solid curve.

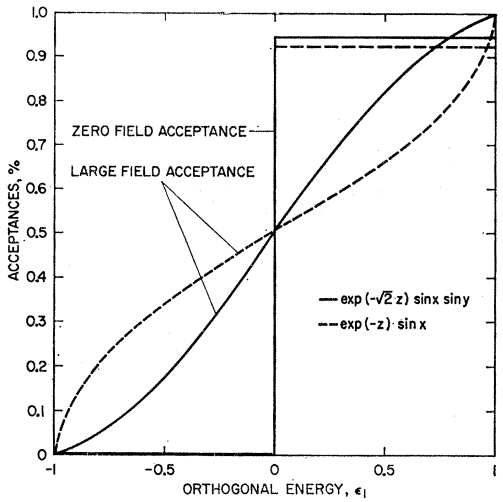

FIG. 8. Acceptance as a function of energy for orthogonal incidence; solid curve, square-checkerboard potential; dashed, stripe-type potential; the large-field acceptances are for the case where the applied electric field far exceeds the patch field and the trajectories may be considered unaffected by the patch field, i.e., undeflected.

VIII. SUMMARY AND DISCUSSION

The reflection coefficient for electrons entering the electric field which originates from the patches of a polycrystalline surface changes abruptly at the threshold of energy from 100% to between 7.7 and 5.4%. This is independent of the detailed nature of the patches, their size, or amplitude. Therefore, high-resolution energy spectrometry with the counterfield method is possible with a patchy counterfield electrode, regardless of the patch amplitude and size.

The angular dependence of the reflection coefficient is calculated and shown in Fig. 4 for a stripe-type potential. The angle of total reflection is found to be slightly more than 20° away from grazing incidence. The reflections are generally nonspecular. From appropriate averaging, we see that electron emission from a patchy surface is anisotropic (i.e., it is deficient in emission parallel to the surface). Because of the patches, the total emission is reduced by about 20% from the emission which a nonpatchy surface would yield. Similar calculations for the more generally applicable checkerboard potential have not been carried out because of the large complication of the problem.[14]

Concerning the reflection coefficient well above threshold, it is interesting to note that negative particles are reflected differently from positive particles if the surface patch potential distribution is nonsymmetric about its zero. For instance, a potential with sharp and narrow positive peaks and broad, shallow, negative

[14] A general idea of the change of the star-shaped area of Fig. 7 for oblique incidence can be obtained by viewing a point source of light through a piece of window glass which has a checkerboard embossment on one surface (such as a bathroom window glass). The distortion of the star when the angle of incidence is varied should be similar to that resulting if the electron optical problem is treated.

valleys such as

$$P(x,z)=\sum_{1}^{n}\cos(\nu x)e^{-\nu z}$$

reflects negative particles only up to a small value of energy, while positive ones are reflected up to much larger energies.

ACKNOWLEDGMENT

Many thanks are due to C. R. Buckey, who guided the author, a novice at the computer, with never-failing patience; who restored the author's self-respect when he lost again and again in arguments with the computer; and who wrote most of the more difficult passages in the programs.

PHYSICAL REVIEW VOLUME 164, NUMBER 3 15 DECEMBER 1967

Angular Forces in the Lattice Dynamics of Face-Centered Cubic Metals

P. S. YUEN AND Y. P. VARSHNI
Department of Physics, University of Ottawa, Ottawa, Canada
(Received 19 June 1967)

The lattice dynamics of the fcc lattice has been investigated using a model in which, in addition to central forces, interatomic forces include angular forces of the type employed by Clark, Gazis, and Wallis. The model has been applied to copper, and results are presented for dispersion curves, vibration spectra, and effective calorimetric and x-ray Debye temperatures.

INTRODUCTION

ANGULAR forces were introduced into lattice dynamics long ago by Born[1] in his treatment of the diamond lattice. However, there have been very few investigations bearing on the applicability or otherwise of the assumption of angular forces in metallic crystals.

Recently, Clark, Gazis, and Wallis[2] have investigated the frequency spectra of bcc lattices using a model in which, in addition to central forces, interatomic forces include angular forces of the type introduced by Gazis, Herman, and Wallis.[3] In the present paper the lattice dynamics of the fcc lattice has been investigated using such a model. An application has been made to copper, for which theoretical and experimental results are compared for dispersion curves, and effective calorimetric and x-ray Debye temperatures.

ANGULAR FORCE MODEL

We consider a monoatomic crystal lattice formed by $(N+1)$ particles. Each particle has a mass M. The potential energy V of the crystal may be expanded in a Taylor series.

In the following, we denote $(\partial^2 V/\partial u_m \partial v_n)_0$ by

$$V\begin{pmatrix}u & v\\ m & n\end{pmatrix};\quad \begin{pmatrix}u=x,y,z;\ v=x,y,z\\ m=0,\cdots,N;\ n=0,\cdots,N\end{pmatrix}.$$

The angular frequencies ω are obtained from the solution of the secular equation[4,5]

$$\left|\sum_n V\begin{pmatrix}u & v\\ 0 & n\end{pmatrix}e^{i2\pi\mathbf{k}\cdot\mathbf{R}_n}-\omega^2 M\delta_{uv}\right|=0, \tag{1}$$

where $\mathbf{R}_n$ is the equilibrium position of the particle n.

For the fcc lattice, we denote the position of a lattice point by

$$\mathbf{R}_{0n}=\mathbf{R}_n=\tfrac{1}{2}a\mathbf{N}_n, \tag{2}$$

where a is the length of one side of the cube. In this notation, (1) becomes

$$\left|\sum_n V\begin{pmatrix}u & v\\ 0 & n\end{pmatrix}e^{i\mathbf{p}\cdot\mathbf{N}_n}-\omega^2 M\delta_{uv}\right|=0, \tag{3}$$

where

$$\mathbf{p}=\pi a\mathbf{k}.$$

The model that we are considering employs central forces between a particle and each of its first and second neighbors, as well as angular forces which depend on the changes of angles in the triangles formed by the particle and its first and second neighbors. This type of angular force has been used by Clark *et al.*[2] The effects of the more distant neighbors are neglected.

Since we only need to use terms of $(\partial^2 V/\partial u_0 \partial v_n)_0$, we can treat the potential energy due to the central force interaction and the angular force interaction separately.

[1] M. Born, Ann. Physik **44**, 605 (1914).
[2] B. C. Clark, D. C. Gazis, and R. F. Wallis, Phys. Rev. **134**, A1486 (1964).
[3] D. C. Gazis, R. Herman, and R. F. Wallis, Phys. Rev. **119**, 533 (1960).
[4] M. Born and K. Huang, *Dynamical Theory of Crystal Lattices* (Oxford University Press, New York, 1962).
[5] R. A. Smith, *Wave Mechanics of Crystalline Solids*, (Chapman and Hall Ltd., London, 1961).